Author's Accepted Manuscript

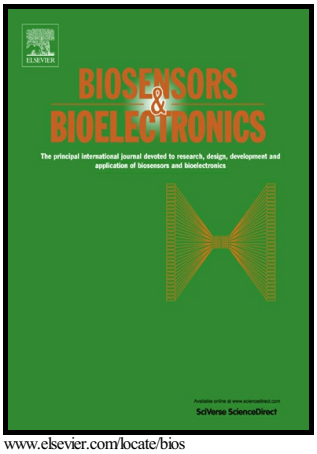

www.elsevier.com/locate/bios

A highly permselective electrochemical glucose sensor using red blood cell membrane

Insu Kim, Dohyung Kwon, Dongtak Lee, Chooga Jeong, Hoon Lee, Gyudo Lee, Dae Sung Yoon

PII: S0956-5663(17)30800-X
DOI: https://doi.org/10.1016/j.bios.2017.12.002
Reference: BIOS10147

To appear in: *Biosensors and Bioelectronic*

Received date: 31 July 2017
Revised date: 22 November 2017
Accepted date: 4 December 2017

Cite this article as: Insu Kim, Dohyung Kwon, Dongtak Lee, Chooga Jeong, Hoon Lee, Gyudo Lee and Dae Sung Yoon, A highly permselective electrochemical glucose sensor using red blood cell membrane, *Biosensors and Bioelectronic,* https://doi.org/10.1016/j.bios.2017.12.002

A highly permselective electrochemical glucose sensor using red blood cell membrane

Insu Kim[a], Dohyung Kwon[a], Dongtak Lee[a], chooga Jeong[b], Hoon Lee[b], Gyudo Lee[a,*], Dae Sung Yoon[a,*]

[a] *School of Biomedical Engineering, Korea University, Seoul 02841, Korea*
[b] *Department of Electrical Engineering, Kwangwoon University, Seoul 01897, Korea*

*E-mail address: dsyoon@korea.ac.kr (D.S.Y.) and lkd0807@korea.ac.kr (G.L.)

Abstract

We developed an electrochemical enzymatic biosensor coated with red blood cell membrane (RBCM) for highly selective glucose measurement. The RBCM containing its membrane proteins (glucose transporter-1) was extracted from a human red blood cell (RBC), and then placed on an established enzymatic glucose sensor by the vesicle fusion method. In the newly fabricated glucose sensor, the RBCM plays the role in the diffusion barrier of preventing the penetration of interfering molecules, while in contrast making glucose molecules permeable. We employed scanning electron microscopy and atomic force microscopy to analyze the RBCM diffusion barriers. The performance of our glucose sensors with diffusion barriers was tested regarding selectivity to glucose against other interfering molecules, such as ascorbic acid, uric acid, and galactose. Remarkably, employing the RBCM significantly improved the selectivity and accuracy of the glucose measurement, even under human serum, compared to the uncoated sensors. This result implies that the RBCM serves well as a highly permselective layer to glucose molecules, and a diffusion barrier to other molecules.

Keywords:
Electrochemical analysis
Glucose biosensor
Glucose dehydrogenase
Red blood cell membrane
Glucose transporter-1
Permselectivity

1. Introduction

Enzymatic electrochemical sensing is typically used in blood glucose sensors, because it results in their high sensitivity, fast response time, and low-cost fabrication (Jia et al. 2016). However, since human blood contains innumerable components, such as proteins, cytokines, blood cells, drug molecules, and ions, the sensors suffer from poor selectivity when measuring whole blood or serum (Croce et al. 2012; Lee et al. 2017). These components, termed interfering species, often interfere with the interactions between glucose and enzymes, resulting in the generation of interfering signals that hinder accurate blood glucose measurements (Vaidya and Wilkins 1994). In this respect, various permselective polymer thin films have been developed to minimize electrochemical interferences from some molecules in blood (Centonze et al. 1994; Palmisano et al. 1993; Palmisano et al. 1994; Zhang et al. 1994). Some permselective polymers, produced by electropolymerization of suited organic molecules, had proved their selectivity to ascorbic acid, uric acid, cysteine, and acetaminophen (Ciriello et al. 2000; Guerrieri et al. 2009; Guerrieri et al. 1998).

Similar to the permselective polymer film, mammal possesses highly permselective system, called blood-brain barrier (BBB) in the brain. BBB's permselective property is based on glucose transporter-1 (GLUT1) expressed on the cell membrane. In general, the cell membrane is well-known as good diffusion barriers to block the penetration of various ions and small hydrophilic molecules (e.g., glucose, galactose, and uric acid) due to the high activation energy of the membrane (Deamer and Bramhall 1986; Finkelstein 1976). The GLUT1, meanwhile, exclusively transport glucose through the cell membrane. As such, among various cell, red blood cell (RBC) express abundant GLUT1 on the cell membrane, which facilitates the diffusion of glucose across the cell membrane (Abbott et al. 2006; Wheeler 1985). Furthermore, RBCs are the most abundant type of blood cells, lacking a nucleus and most organelles, and their plasma membranes are highly biocompatible (Gao et al. 2013; Ji et al. 2011). In this respect, the red blood cell membrane (RBCM) is suitable for the fabrication of diffusion barriers. Employing RBCM as a permselective layer in a glucose sensor is thought to be one of the most intriguing approaches to improve the selectivity of the sensor. To our best knowledge, this is the first report that deals with the improvement of device performance by implementing the permselective layer using the RBCM. This approach may be appreciable to designing biocompatible, hemocompatible, and immune

evasive glucose biosensor toward next-generation implantable and transdermal glucose monitoring devices (Dehaini et al. 2017; Fang et al. 2013; Fang et al. 2015; Kim et al. 2011; Lee et al. 2016).

In this study, we developed an electrochemical enzymatic biosensor coated with RBCM for highly selective glucose measurement. Fig. 1a shows a schematic of working mechanism. The RBCM and its membrane proteins were extracted from human RBC. After ultrasonication, the RBC extracts were placed on established enzymatic glucose sensors by the vesicle fusion method to form permselective layers that possessed GLUT1. The permselective layers fabricated on the device were analyzed by stylus profiler, Fourier transform infrared spectroscopy (FT-IR), dynamic light scattering (DLS), scanning electron microscopy (SEM), and atomic force microscopy (AFM). The performance of our glucose sensors using glucose dehydrogenase with RBCM was tested regarding selectivity to glucose; specifically, whether they responded to other interfering molecules, such as ascorbic acid, uric acid, and galactose (Fig. 1a). Moreover, we discuss several advantages of our method from the viewpoint of the practical use of glucose sensors.

2. Experimental method

2.1. Chemicals HK buy

D-(+)-Glucose, ascorbic acid, uric acid, galactose, sodium phosphate dibasic, sodium phosphate monobasic, human serum (from human male AB plasma), and glucose hexokinase kit were purchased from Sigma-Aldrich. Phospholipid, 1,2-dipalmitoyl-sn-glycero-3-phosphocholine (DPPC), was purchased from Avanti Polar Lipid. Electrode strips (Roche, ACCU-CHEK Performa) were purchased from Roche. Distilled water was purchased from Gibco, and used in each solution. A 0.1 M phosphate buffer solution (PBS) was prepared by adding aqueous solutions of 0.1 M sodium phosphate dibasic into a 0.1 M sodium phosphate monobasic, until a pH of 7.4 was achieved. All the reagents were dissolved in a 0.1 M PBS for measurement. A glucose stock solution (40 mM) was prepared, and preserved in a refrigerator at 4°C. The solutions of ascorbic acid, uric acid, and galactose were freshly prepared before use.

2.2. Apparatus and measurements

The morphologies of the uncoated sensor and the RBCM-coated sensor (RBCM sensor) were examined by scanning electron microscopy (SEM, JSM-6701F, JEOL) with high voltage (10 kV). The surface topologies of the uncoated and RBCM sensor were measured by atomic force microscopy (AFM, Innova, Bruker). The surface roughness and thickness (height) of a single layer of RBCM were calculated using NanoScope Analysis software. Chronoamperometry was performed using a potentiostat (Versastat3, AMETEK) controlled by VersaStudio software. All of the chronoamperometry was conducted at a potential of -0.3 V at room temperature. The detection potential was empirically chosen by measuring the cyclic voltammetry. Briefly, at -0.3 V the sensing performance of our glucose sensor was greater than the noise signal in the absence of glucose. Cyclic voltammetry was conducted from -0.6 to 0 V at 50 mV/s speed. Electrochemical impedance spectroscopy (EIS) was conducted at -0.3 V potential from 0.5 to 10k Hz with 0.1 M PBS and 5 mM glucose. The RBCM extracted from the RBC was examined by attenuated total refractive Fourier transform infrared spectroscopy (ATR-FTIR, spectrum 100, Perkin Elmer). The hydrodynamic diameters of the sonicated RBCM vesicles were verified by dynamic light scattering (DLS, Zetasizer S90, Malvern). The thickness of the RBCM layer was measured by stylus profiler (Alpha-step D100, KLA-Tencor).

2.3. Red blood cell membrane collection

RBCs were extracted from human whole blood using a protocol described previously (Gao et al. 2013). In detail, whole blood was drawn into an EDTA tube from a healthy 24-year-old male. The whole blood was centrifuged at 1,000 g for 5 min at 4°C to isolate the RBCs from the plasma and buffy coats. The resulting precipitate, RBCs, was collected, and washed three times with 1× PBS (pH 7.4, Gibco) at 4°C, before hemolysis. The washed RBCs were suspended in 0.25× PBS for 20 min at 4°C for hemolysis. Following the hemolysis, hemoglobins and peripheral membrane proteins were released into solution. The hemolyzed solution was centrifuged at 1,000 g for 5 min to separate the cytoplasmic components and peripheral membrane proteins from the RBCM. The supernatant was removed, and the pellet of RBCM was washed twice with 1× PBS at 4°C. The resulting RBCM was inspected by

ATR-FTIR spectrometry (Fig. S1). More detailed information and explanation are available in the Supplementary Materials.

2.4. Fabrication of the RBCM sensor and its optimization

The electrode was purchased from Roche. The working electrode, counter electrode, and reference electrode were composed of gold (Fig. 1b). Each of the electrodes was screen-printed on a polymer substrate. The enzyme composite consisted of quinoprotein glucose dehydrogenase (GDH), pyrroloquinoline (PQQ), mediator, buffer, and non-reactive ingredients in a fixed ratio (Fig. S2). The enzyme composite was cast on the electrode (~33 mm^2), and dried. Detailed enzymatic reactions for glucose sensing are provided in the next section. The permselective RBCM was evenly deposited on the electrode by a vesicle fusion method (Fig. 1c) (Castellana and Cremer 2006). Specifically, 2.5 μl of the RBCM solution was diluted with 1 ml of 0.1 M PBS, 0.25% (v/v). Before the deposition of RBCM, the diluted RBCM solution was sonicated for 30 min to form 170 nm sized RBCM vesicles that are thermodynamically easy to fuse to the electrode (Fig. S3) (Mingeot-Leclercq et al. 2008). An RBCM vesicle suspension of 25 μl was dispensed on the electrode to cover the enzyme complexes. All of the electrodes were incubated in a drying oven at 50°C for 50 min. The enzyme activity of GDH is retained up to 65°C (Yamazaki et al. 1999). After the incubation, the RBCM sensors were allowed to cool at room temperature for 50 min. The surface roughness and thickness of the deposited RBCM layer were investigated using the AFM and the stylus profiler. DPPC, the major component of phospholipid membrane without GLUT1, was sonicated and dispensed on the electrode in the same procedure with RBCM.

2.5. Measurement of glucose by quinoprotein glucose dehydrogenase

Quinoprotein glucose dehydrogenase (GDH-PQQ) was used in our sensors as a biological element and a transducer. Although its specificity toward glucose is less than that of glucose oxidase, the thermal denaturation temperature of PDH-PQQ is more appropriate for our RBCM coating process (Yamazaki et al. 1999). Dehydrogenase and quinoprotein acted as an enzyme and cofactor, respectively. GDH-PQQ requires mediators to assist the redox process

(Fig. S4). The chemical equation of GDH-PQQ to generate electrical signals is as follows (Fender et al. 2012):

$$\mathrm{D-Glucose + GDH-PQQ_{Ox} \rightarrow D-Glucono-1,5-lactone + GDH-PQQ_{Re}} \quad (1)$$

$$\mathrm{GDH-PQQ_{Re} + Mediator_{Ox} \rightarrow GDH-PQQ_{Ox} + Mediator_{Re}} \quad (2)$$

where, the subscript *Ox* represents the oxidized form, while the subscript *Re* represents the reduced form.

In Eq. 2, the final product, reduced mediator, generates electrical signals by oxidation. The restricted amount of mediator in the enzyme complex leads to enzyme reactions, until all the mediators are consumed. The Michaelis-Menten kinetics model for a single-substrate reaction was employed for the enzyme assay (Lee et al. 2012b; Orosco et al. 2009). The kinetics enables the measurement of the diffusion rate to discriminate the concentration of the substrate (i.e., glucose). We could calculate the diffusion rate of glucose empirically over a range of 3 to 7 s. For validation of our method, glucose hexokinase assay, one of the standard glucose tests, was performed at the same condition (Fig. S5)(Theuer et al. 2017; Tric et al. 2017).

2.6. Schematic design of the RBCM sensor

Fig. 1a illustrates the concept of the working mechanism of the RBCM sensor. The RBCM is multilayered onto the enzyme complex layer to form a permselective diffusion barrier. The RBCM exclusively facilitate the diffusion of glucose through the GLUT1 of RBCM; the inset box (bottom right) depicts the working model of GLUT1 with three different types of conformations (Deng et al. 2014). In contrast, typical interfering molecules in the blood, such as ascorbic acid (AA), uric acid (UA), and galactose (GA), are blocked by the appropriate thickness of the RBCM layer (see Fig. 2). By taking advantages of RBCM and its GLUT1, we realize molecular permselectivity.

3. Results and discussion

3.1. Optimization of concentration of the RBCM

For reliable operation of our device, we need to optimize the fabrication condition of the RBCM. It is believed that the RBCM on the device must have a uniform surface and more importantly, an appropriate thickness. In other words, because glucose molecules are transported through the diffusion process, there exists an optimal diffusion layer thickness that produces a better sensor signal. We prepared three concentrations of RBCM suspensions by diluting 1, 2.5, and 5 μl of RBCM suspensions with 1 ml of 0.1 M PBS; the volume concentration of each suspension is adjusted to 0.1, 0.25, and 0.5 vol%, respectively. Each of the diluted suspensions was deposited on the uncoated sensors, and then the device was incubated at 50°C for 50 min in a dry oven. The thickness of the RBCM layer was measured with a stylus profiler (Fig. 2a) (Son and Butler 2015). It was found that the thickness is proportional to the volume concentration of the suspension. The approximate thickness of the RBCM layer was measured to be 85 ± 22, 203 ± 40, and 440 ± 51 nm for 0.1, 0.25, and 0.5 vol% RBCM suspensions, respectively. Further AFM analysis revealed that the thickness of a single layer of RBCM was about 5 nm (Fig. S6). We speculated that the number of individual layer of the RBCM was approximately 17 ± 4, 40 ± 10, and 88 ± 12 layers at 0.1, 0.25, and 0.5 vol% RBCM suspensions, respectively.

The sensors with RBCM layers of different thicknesses were used to measure the current when exposed to 10 mM glucose solution. The results reveal that each device with different RBCM thickness shows different modality (diffusion stability) in its diffusion kinetics (Fig. 2b, c, and S7). The device with 85-nm-thick RBCM layer displayed the fastest diffusion rate among the three, but lacked linearity in the diffusion. This was due to the rough and porous structure of the enzyme-casted surface, where the 85-nm-thick RBCM layer was not sufficient to fully cover the surface (see Fig. 3a). Accordingly, a significant amount of glucose could easily penetrate through the layer, without the aid of GLUT1. On the other hand, the device with 203-nm-thick RBCM layer exhibited excellent linearity and a steady diffusion over 10 s. However, for the 440-nm-thick RBCM, the linear range of the diffusion became narrow, indicating that the excessively thick layer retarded the facilitated diffusion of glucose by GLUT1. Based on the above result, we optimized the thickness of RBCM layer by ~200 nm for our further experiments. Because there exists the slope dependence by RBCM thickness and stability, possibly resulting in some errors, careful control of the RBCM thickness and stability should be required for better accuracy. Data in the range of 1–10 s

were fitted by linear regression equation for the reference value. The R-square values were estimated to be 0.941, 0.997, and 0.967 for the 85, 203, and 440 nm RBCM layers, respectively.

3.2. Visualization of the surface of the RBCM-coated sensor

To investigate the microstructure of the RBCM sensor, we conducted structural analysis using SEM and AFM. Fig. 3a and b show the SEM images of the surface morphologies of both the RBCM sensor, and the uncoated sensor on the devices. The uncoated sensor has a composite structure that is composed of an enzyme and non-reactive ingredients on Au electrode. In particular, the enzyme complex layer shows a porous structure that helps the analyte permeate into the electrode (Fig. 3a). However, after the coating of the RBCM, the RBCM sensor displays a very smooth surface with no pores (Fig. 3b). This indicates that the RBCM suspension completely covers the porous structure, and forms a multi-layered RBCM structure.

For detailed analysis, the surface roughness of both the RBCM sensor and the uncoated sensor was measured by AFM (Fig. 3c and d). At the projected area of 400 μm2 (20 × 20 μm^2), both the RBCM and the uncoated sensors were scanned by AFM probe to collect topographic data. The surface roughness (R_q) was calculated from the topographic data, where Rq represents the root mean square average of the height deviations (Z) estimated from the sample image as per the following equation (Lee et al. 2012a):

$$R_q = \sqrt{\frac{\sum (Z_i)^2}{N}} \qquad (3)$$

The calculated R_q value of the surface of the uncoated sensor (the enzyme complex layer) was ~86.7 ± 21.4 nm, which is approximately eight times greater than that of the RBCM layer (~11.2 ± 0.9 nm). The histogram of the height distributions revealed a similar trend; the distribution narrowed, since the RBCM was coated on the electrode (Lee et al. 2012a) (Fig. 3e and 3f). The AFM result is consistent with that of the SEM analysis. Both the analyses suggest that the RBCM has a smooth surface and consists of a multi-layered structure. For glucose sensing, the analyte should penetrate the thick multi-layered membrane structure. Accordingly, it is considered that this RBCM structure can serve as a diffusion barrier that is penetrated by glucose molecules only.

3.3. Electrochemical glucose detection using the RBCM sensor

We investigated the performance of RBCM sensors on the glucose concentration. An electrochemical analysis using chronoamperometry was conducted for each glucose concentration in the glucose range of human blood (2.5 to 40 mM). At each measurement, 30 μl of the glucose solution was dropped on an electrode, and the measurement ran for 10 s at a -0.3 V detection potential. We set the potential as -0.3 V by conducting cyclic voltammetry (Fig. S8). The measured chronoamperogram was displayed on a logarithmic scale. Then, the slope (Δoutput current in Fig. 4, 5, and 6) was calculated over the time range of 3–7 s. Fig. 4 shows the calibration curves of the uncoated, the RBCM, and the DPPC-coated glucose sensors (DPPC sensor) at different glucose concentrations (2.5 to 40 mM). Note that the DPPC sensor was used as a control sample to verify whether the DPPC without GLUT1 effectively acted as a molecular diffusion barrier to hinder the penetration of all hydrophilic molecules or ions. Fig. 4a shows the plots that were fitted by the Michaelis-Menten equation for a single substrate. The maximum diffusion rate (V_{max}) was measured to be 54.5, 55.2, and 3.11 μM/s, while the Michaelis constant (K_m) was measured to be 12.4, 11.9, and 0.18 mM for the uncoated, the RBCM, and the DPPC sensors, respectively. Fig. 4b reveals the detailed information at the measurement range of 2.5 to 10 mM, which corresponds to the blood glucose level of both normal and diabetes patients (Al-Sagur et al. 2017; Li et al. 2017; Ribet et al. 2017). Data in the range were fitted by linear regression equation. The linearity (i.e., R-square) values for the uncoated, RBCM, and DPPC sensors were estimated to be 0.994, 0.996, and 0.797, respectively. It was confirmed that our RBCM sensors exhibited an excellent linearity in the concentration range of 0–10 mM. In the case of the abnormal glucose concentration (>10 mM) far beyond the normal, proper dilution of the sample might help one to conduct more accurate measurement. That is because its final concentration after proper dilution would fit within the linear range of our sensors.

Compared to the RBCM sensor, no significant signals were measured in the case of the DPPC sensor at any concentration of glucose, indicating that the DPPC sensor retained no permeability. Moreover, the limit of detection (LOD) of the RBCM sensors (1.06 mM) was slightly improved, compared to the uncoated sensors (1.34 mM). This may be attributed to the role of the RBCM as a permselective layer that can impede both the diffusion of other

molecules, and interference with the electrode (Sin et al. 2014). The results corresponded to our EIS results that the electron transfer of RBCM sensor was slightly enhanced compared with that of the uncoated sensor in the presence of glucose (Fig. S9). In addition, we validated whether the sensing performance of the RBCM glucose sensors was sustainable three weeks after fabrication (Fig. S10). We measured the output signals of both the fresh and the 3-week stored sensors, and calculated the mean difference (Δm) in output signal between the sensors. The results show that the RBCM sensors revealed highly stable output signals (Δm = ~0.21 μA/s) at 5 mM glucose; whereas, after three weeks, the uncoated sensors exhibited drifts in the output signal (Δm = ~0.81 μA/s). This indicates that the RBCM works well not only for the glucose-specific permselective layer, but also as a protection layer that can prevent the denaturation of enzyme complexes by absorbing humidity. These combined results suggest that our condition for fabricating the RBCM is well optimized.

3.4. Selectivity test of RBCM-coated sensors

Next, we conducted selectivity tests of the RBCM glucose sensors to ascorbic acid (AA), uric acid (UA), and galactose (GA) molecules by chronoamperometry. AA and UA are antioxidants that can interfere with electrochemical sensing. GA is a stereoisomer of glucose that has the same molecular formula and sequence of bonded atoms; it tends to be misidentified as glucose by glucose dehydrogenase (Flexer et al. 2008; Schleis 2007). For the selectivity test, various mixture solutions (100, 200, 300, and 400 μM AA, UA, or GA) were made by adding different amounts of molecules into 5 mM glucose solutions. Note that the concentration range of each source in the mixture solution was determined by referring to its normal range in human blood. The electrochemical signal of the glucose sensor was measured when each mixture solution was injected. Fig. 5 demonstrates the measured signals of both the uncoated and the RBCM sensors at each concentration of the three types of molecules. Surprisingly, all three sources (AA, UA, and GA) hardly interfered with the electrochemical signals of the RBCM sensors, exhibiting very low signal drifts (σ = 0.18, 0.14, and 0.09 μA/s, respectively) over the whole concentration range (Fig. S11). In contrast, the uncoated sensors displayed very high drifts in signal (σ = 0.63, 1.68 and 0.96 μA/s, respectively), depending on the concentration of the interfering molecules. In addition, the percentage error (%error) of each result was calculated (Fig. S12). It is shown that most

results of RBCM sensors exhibit much less %error in glucose measurement on the samples containing three different types of molecules than that of the uncoated sensors.

Interestingly, in the case of the uncoated sensors, the output signal decreased with the concentration of UA or GA, but conversely, increased with AA. This implies that the characteristic of the interfering signal is strongly dependent on the type of interfering molecules for the uncoated sensor (Gopalan et al. 2016). Also, a mixture of three interfering molecules (100 μM of AA, UA, and GA) in 5 mM glucose solution was also used for the selectivity test (Fig. S13). The result of the test indicates that the diffusion rate of the uncoated sensor was highly affected by these interfering molecules. By contrast, the RBCM effectively prevented the penetration of these interfering molecules, exhibiting reliable output signals, regardless of their concentrations.

Ultimately, Fig. 6 shows the results of the selectivity test of the RBCM glucose sensors, which was conducted using human serum samples (pH 7.4, see specifications in Fig. S14) with the addition of glucose (0 to 4 mM). Compared to the PBS sample, human serum contains innumerable interfering species (not only AA, UA, and GA, but also other proteins, ions, or lipids) that would hamper the enzymatic redox reactions between glucose and the enzymes on the electrodes (Krebs 1950). Therefore, this test is a more comprehensive estimation regarding whether the RBCM sensors can work stably and similarly with the device performance revealed in PBS. Surprisingly, the RBCM glucose sensor exhibited very stable output in serum solutions. The RBCM sensor still retained a good linearity (0.9991) and the signal's slope increased by only 5%, whereas the uncoated sensor exhibited a relatively poor linearity (0.9769) and the signal's slope decreased by 30%. The LOD of the RBCM sensor was 1.11 mM in serum solutions, which is comparable to that (1.06 mM) of the test conducted in PBS. Contrary to the RBCM sensor, the LOD of the uncoated sensor was significantly worsened (2.51 mM in serum), and nearly two times higher than that (1.34 mM) of the test conducted in PBS. More remarkably, by employing the RBCM, the signal increment between two neighboring concentrations was significantly accurate (4.1~13.6% in %error) in serum samples, compared to the uncoated sensor (7.2~52.2% in %error). This result provides more realistic evidence for the superior selectivity performance of our RBCM-based glucose sensors and reveals a strong potential for the practical use.

Despite the strong advantages of our sensors, they also have some limitations that should be solved through scientific approaches. Here, we used permselective layers (RBCM) extracted from human RBC, which may represent limitations for massive production of the RBCM sensor. One of the solutions would be to use carcinoma cell line such as MDA-MB-231 because they also express a large amount of GLUT1 on their plasma membrane (Venturelli et al. 2016). Unlike RBC, carcinoma cell line can be easily cultured, genetically modified for greater expression of GLUT1, and more precisely optimized for various conditions. Also, our sensor was designed to be the disposable form using three electrodes made of the same material (*i.e.*, gold) that might lead potential drift with low stability (Shinwari et al. 2010). Further study would be necessary to develop reusable RBCM-based permselective glucose sensors by proper tuning of the electrode modification such as electrode design and material selection.

4. Conclusions

In summary, we propose an electrochemical glucose biosensor that takes advantage of the RBCM as a glucose-specific permselective layer and a diffusion barrier to other interfering molecules. It was found that the RBCM played an important role as a highly stable biological filter against the predominant interfering molecules in blood, such as AA, UA, and GA. The unique structure of the RBCM (lipid bilayer containing abundant GLUT1) made it possible to penetrate glucose molecules across the RBCM, while preventing the penetration of other interfering molecules. Through this mechanism, the diffused glucose molecules can approach the enzyme complexes on the electrode, where they are involved in redox reactions to produce an electrochemical signal. Nevertheless, it was found that either the considerably thinner (<<200 nm) or thicker (>>200 nm) RBCM exhibited poor or delayed diffusion of glucose, although the GLUT1 facilitated the diffusion of glucose. From the experiment, we obtained the optimal thickness (~200 nm) of the RBCM that effectively restricted the penetration of interfering molecules, while simultaneously minimizing the delay of glucose diffusion. Remarkably, the optimized RBCM glucose sensors worked well, even in serum condition, showing good reliability at various glucose concentrations which are further provided, ranging from 0 to 4 mM, into the human serum. We also confirmed the long-term stability of our RBCM sensors for glucose measurement for at least three weeks. Taken

together, our results provide a new insight that RBCM may be a promising material to improve the performance of glucose sensors in terms of selectivity and accuracy.

Acknowledgements

This work was supported by the National Research Foundation of Korea (NRF) Grant, funded by the Korean Government (MSIP) (No. NRF-2016R1A2B4010269).

References

Abbott, N.J., Ronnback, L., Hansson, E., 2006. Astrocyte-endothelial interactions at the blood-brain barrier. Nat. Rev. Neurosci. 7(1), 41-53.

Al-Sagur, H., Komathi, S., Khan, M.A., Gurek, A.G., Hassan, A., 2017. A novel glucose sensor using lutetium phthalocyanine as redox mediator in reduced graphene oxide conducting polymer multifunctional hydrogel. Biosens. Bioelectron. 92(Supplement C), 638-645.

Castellana, E.T., Cremer, P.S., 2006. Solid supported lipid bilayers: From biophysical studies to sensor design. Surface Science Reports 61(10), 429-444.

Centonze, D., Guerrieri, A., Palmisano, F., Torsi, L., Zambonin, P.G., 1994. Electrochemically prepared glucose biosensors: kinetic and faradaic processes involving ascorbic acid and role of the electropolymerized film in preventing electrode-fouling. Fresenius' Journal of Analytical Chemistry 349(7), 497-501.

Ciriello, R., Cataldi, T.R.I., Centonze, D., Guerrieri, A., 2000. Permselective Behavior of an Electrosynthesized, Nonconducting Thin Film of Poly(2-naphthol) and Its Application to Enzyme Immobilization. Electroanalysis 12(11), 825-830.

Croce, R.A., Vaddiraju, S., Papadimitrakopoulos, F., Jain, F.C., 2012. Theoretical Analysis of the Performance of Glucose Sensors with Layer-by-Layer Assembled Outer Membranes. Sensors 12(10), 13402.

Deamer, D.W., Bramhall, J., 1986. Permeability of lipid bilayers to water and ionic solutes. Chem. Phys. Lipids 40(2), 167-188.

Dehaini, D., Wei, X., Fang, R.H., Masson, S., Angsantikul, P., Luk, B.T., Zhang, Y., Ying, M., Jiang, Y., Kroll, A.V., Gao, W., Zhang, L., 2017. Erythrocyte–Platelet Hybrid Membrane Coating for Enhanced Nanoparticle Functionalization. Adv. Mater. 29(16), 1606209-n/a.

Deng, D., Xu, C., Sun, P., Wu, J., Yan, C., Hu, M., Yan, N., 2014. Crystal structure of the human glucose transporter GLUT1. Nature 510(7503), 121-125.

Fang, R.H., Hu, C.-M.J., Chen, K.N.H., Luk, B.T., Carpenter, C.W., Gao, W., Li, S., Zhang, D.-E., Lu, W., Zhang, L., 2013. Lipid-insertion enables targeting functionalization of erythrocyte membrane-cloaked nanoparticles. Nanoscale 5(19), 8884-8888.

Fang, R.H., Luk, B.T., Hu, C.-M.J., Zhang, L., 2015. Engineered nanoparticles mimicking cell membranes for toxin neutralization. Advanced Drug Delivery Reviews 90, 69-80.

Fender, J.E., Bender, C.M., Stella, N.A., Lahr, R.M., Kalivoda, E.J., Shanks, R.M.Q., 2012. Serratia marcescens Quinoprotein Glucose Dehydrogenase Activity Mediates Medium Acidification and Inhibition of Prodigiosin Production by Glucose. Appl. Environ. Microbiol.

78(17), 6225-6235.
Finkelstein, A., 1976. Water and nonelectrolyte permeability of lipid bilayer membranes. J. Gen. Physiol. 68(2), 127-135.
Flexer, V., Ielmini, M.V., Calvo, E.J., Bartlett, P.N., 2008. Extracting kinetic parameters for homogeneous [Os(bpy)(2)ClPyCOOH](+) mediated enzyme reactions from cyclic voltammetry and simulations. Bioelectrochemistry 74(1), 201-209.
Gao, W., Hu, C.-M.J., Fang, R.H., Luk, B.T., Su, J., Zhang, L., 2013. Surface Functionalization of Gold Nanoparticles with Red Blood Cell Membranes. Adv. Mater. 25(26), 3549-3553.
Gopalan, A.I., Muthuchamy, N., Komathi, S., Lee, K.P., 2016. A novel multicomponent redox polymer nanobead based high performance non-enzymatic glucose sensor. Biosens. Bioelectron. 84, 53-63.
Guerrieri, A., Ciriello, R., Centonze, D., 2009. Permselective and enzyme-entrapping behaviours of an electropolymerized, non-conducting, poly(o-aminophenol) thin film-modified electrode: A critical study. Biosens. Bioelectron. 24(6), 1550-1556.
Guerrieri, A., De Benedetto, G.E., Palmisano, F., Zambonin, P.G., 1998. Electrosynthesized non-conducting polymers as permselective membranes in amperometric enzyme electrodes: a glucose biosensor based on a co-crosslinked glucose oxidase/overoxidized polypyrrole bilayer. Biosens. Bioelectron. 13(1), 103-112.
Ji, P., Murata-Hori, M., Lodish, H.F., 2011. Formation of mammalian erythrocytes: chromatin condensation and enucleation. Trends Cell Biol. 21(7), 409-415.
Jia, X., Dong, S., Wang, E., 2016. Engineering the bioelectrochemical interface using functional nanomaterials and microchip technique toward sensitive and portable electrochemical biosensors. Biosens. Bioelectron. 76, 80-90.
Kim, S., Oh, W.-K., Jeong, Y.S., Hong, J.-Y., Cho, B.-R., Hahn, J.-S., Jang, J., 2011. Cytotoxicity of, and innate immune response to, size-controlled polypyrrole nanoparticles in mammalian cells. Biomaterials 32(9), 2342-2350.
Krebs, H.A., 1950. Chemical Composition of Blood Plasma and Serum. Annual Review of Biochemistry 19(1), 409-430.
Lee, G., Eom, K., Park, J., Yang, J., Haam, S., Huh, Y.-M., Ryu, J.K., Kim, N.H., Yook, J.I., Lee, S.W., Yoon, D.S., Kwon, T., 2012a. Real-Time Quantitative Monitoring of Specific Peptide Cleavage by a Proteinase for Cancer Diagnosis. Angew. Chem. 124(24), 5939-5943.
Lee, G., Park, I., Kwon, K., Kwon, T., Seo, J., Chang, W.-J., Nam, H., Cha, G.S., Choi, M.H., Yoon, D.S., Lee, S.W., 2012b. Electrochemical detection of high-sensitivity CRP inside a microfluidic device by numerical and experimental studies. Biomed. Microdevices 14(2), 375-384.
Lee, H., Choi, T.K., Lee, Y.B., Cho, H.R., Ghaffari, R., Wang, L., Choi, H.J., Chung, T.D., Lu, N., Hyeon, T., Choi, S.H., Kim, D.-H., 2016. A graphene-based electrochemical device with thermoresponsive microneedles for diabetes monitoring and therapy 11, 566.
Lee, H., Kim, H., Han, H., Lee, M., Lee, S., Yoo, H., Chang, J.H., Kim, H., 2017. Microbubbles used for contrast enhanced ultrasound and theragnosis: a review of principles to applications. Biomed. Eng. Lett., 1-11.
Li, H., Liu, C., Wang, D., Zhang, C., 2017. Chemiluminescence cloth-based glucose test sensors (CCGTSs): A new class of chemiluminescence glucose sensors. Biosens. Bioelectron. 91(Supplement C), 268-275.
Mingeot-Leclercq, M.-P., Deleu, M., Brasseur, R., Dufrene, Y.F., 2008. Atomic force microscopy of supported lipid bilayers. Nat. Protoc. 3(10), 1654-1659.

Orosco, M.M., Pacholski, C., Sailor, M.J., 2009. Real-time monitoring of enzyme activity in a mesoporous silicon double layer. Nat. Nanotechnol. 4(4), 255-258.
Palmisano, F., Centonze, D., Guerrieri, A., Zambonin, P.G., 1993. An interference-free biosensor based on glucose oxidase electrochemically immobilized in a non-conducting poly(pyrrole) film for continuous subcutaneous monitoring of glucose through microdialysis sampling. Biosens. Bioelectron. 8(9), 393-399.
Palmisano, F., Centonze, D., Zambonin, P.G., 1994. An in situ electrosynthesized amperometric biosensor based on lactate oxidase immobilized in a poly-o-phenylenediamine film: determination of lactate in serum by flow injection analysis. Biosens. Bioelectron. 9(7), 471-479.
Ribet, F., Stemme, G., Roxhed, N., 2017. Ultra-miniaturization of a planar amperometric sensor targeting continuous intradermal glucose monitoring. Biosens. Bioelectron. 90(Supplement C), 577-583.
Schleis, T.G., 2007. Interference of Maltose, Icodextrin, Galactose, or Xylose with Some Blood Glucose Monitoring Systems. Pharmacotherapy 27(9), 1313-1321.
Shinwari, M.W., Zhitomirsky, D., Deen, I.A., Selvaganapathy, P.R., Deen, M.J., Landheer, D., 2010. Microfabricated Reference Electrodes and their Biosensing Applications. Sensors 10(3), 1679.
Son, S., Butler, P.J., 2015. Lipid bilayer control of nascent adhesion formation. Biomed. Eng. Lett. 5(3), 172-180.
Theuer, L., Lehmann, M., Junne, S., Neubauer, P., Birkholz, M., 2017. Micro-Electromechanical Affinity Sensor for the Monitoring of Glucose in Bioprocess Media. International Journal of Molecular Sciences 18(6), 1235.
Tric, M., Lederle, M., Neuner, L., Dolgowjasow, I., Wiedemann, P., Wölfl, S., Werner, T., 2017. Optical biosensor optimized for continuous in-line glucose monitoring in animal cell culture. Analytical and Bioanalytical Chemistry 409(24), 5711-5721.
Vaidya, R., Wilkins, E., 1994. Effect of interference on amperometric glucose biosensors with cellulose acetate membranes. Electroanalysis 6(8), 677-682.
Venturelli, L., Nappini, S., Bulfoni, M., Gianfranceschi, G., Dal Zilio, S., Coceano, G., Del Ben, F., Turetta, M., Scoles, G., Vaccari, L., Cesselli, D., Cojoc, D., 2016. Glucose is a key driver for GLUT1-mediated nanoparticles internalization in breast cancer cells 6, 21629.
Wheeler, T.J., 1985. The Glucose Transporter of Mammalian Cells. Annu. Rev. Physiol. 47(1), 503-517.
Yamazaki, T., Tsugawa, W., Sode, K., 1999. Increased thermal stability of glucose dehydrogenase by cross-linking chemical modification. Biotechnology Letters 21(3), 199-202.
Zhang, Y., Hu, Y., Wilson, G.S., Moatti-Sirat, D., Poitout, V., Reach, G., 1994. Elimination of the Acetaminophen Interference in an Implantable Glucose Sensor. Analytical Chemistry 66(7), 1183-1188.

Figures and captions

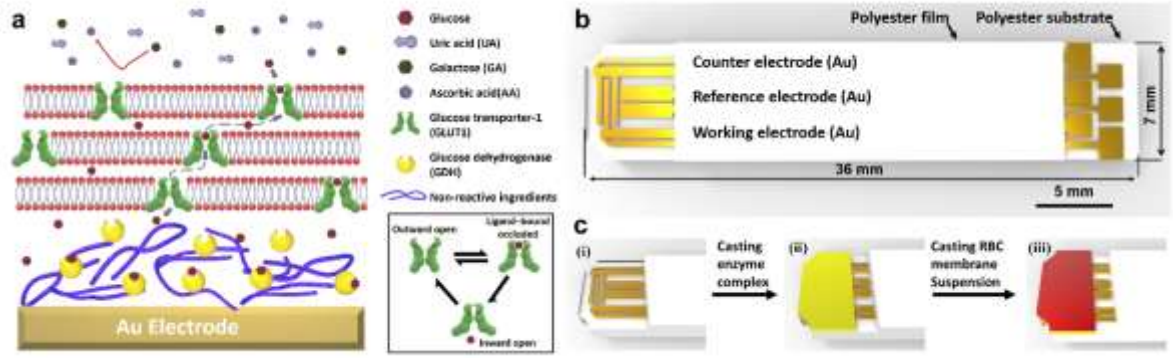

Fig. 1. a) Schematic illustration of the RBCM sensor. The RBCM layer acts as a diffusion barrier to hinder the penetration of interfering molecules (AA, UA, and GA) except for glucose. The GLUT1, incorporated into the RBCM, facilitates the diffusion of glucose molecules through the RBCM. The diffused glucose molecules react with glucose dehydrogenases to produce electrons. Inset box represents the conformational changes of GLUT1. b) Schematic image depicting the structure of an electrode substrate. c) The fabrication process of the RBCM sensor: (i) Au-screen printed electrode; (ii) enzyme mixture-casted Au electrode; and (iii) RBCM-coated enzyme/Au electrode. The area of the fabrication of the enzyme mixture and RBCM is estimated to be ~33 mm^2.

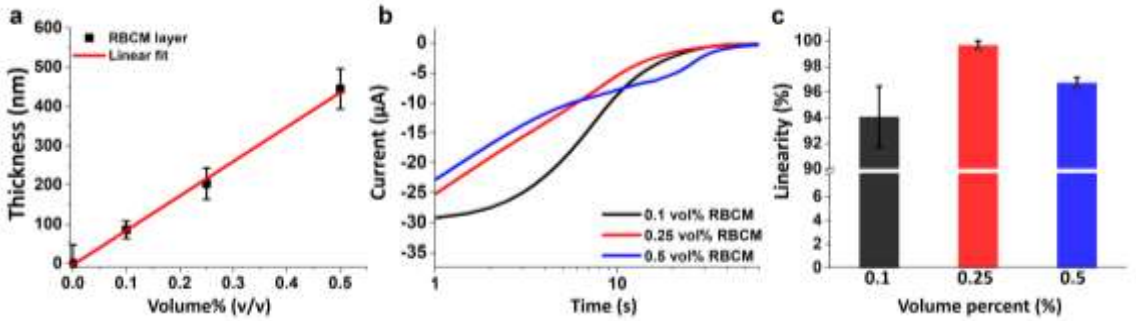

Fig. 2. a) RBCM thickness with different concentrations of RBCM suspension. Approximately 85, 203, and 440 nm at 0.1, 0.25, and 0.5 vol%. b) Amperometric responses from 10 mM glucose with different RBCM thicknesses c) Linearity of the amperometric response of each thickness of RBCM, which is calculated from the data (b) by fitting each curve in a particular time range from 1 to 10 s.

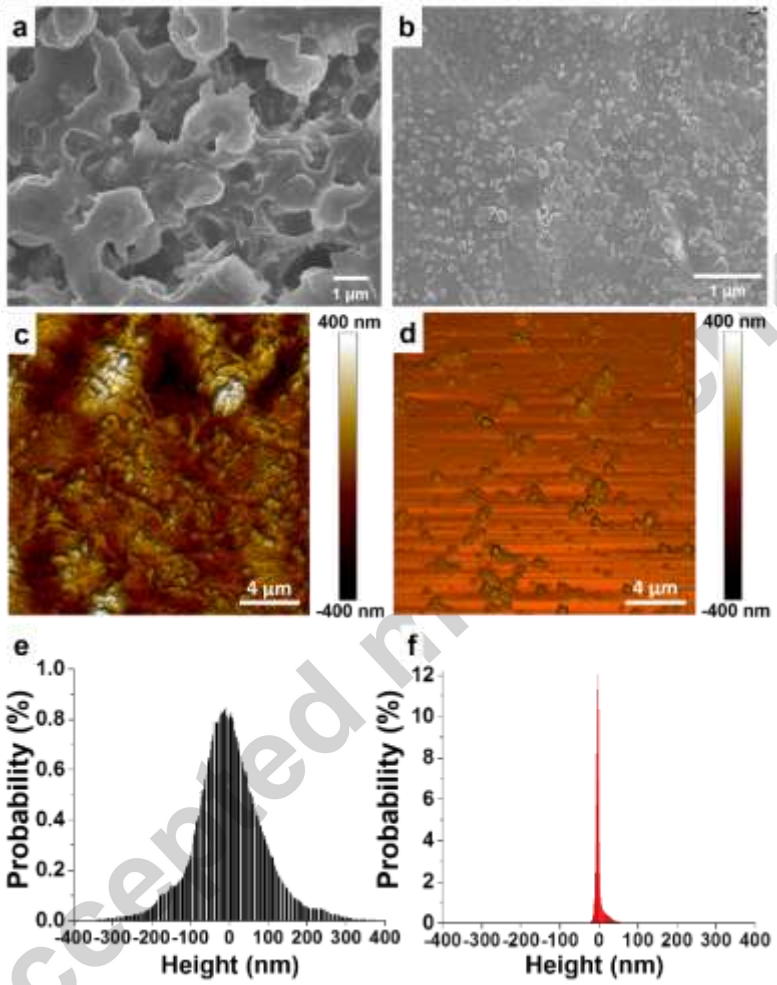

Fig. 3. SEM images of a) uncoated (enzyme complex) and b) RBCM sensor. AFM topographic images of c) uncoated and d) RBCM sensor (image size: 20 × 20 µm^2). Height distribution of e) uncoated and f) RBCM sensor, calculated from the AFM topographic images (c, d).

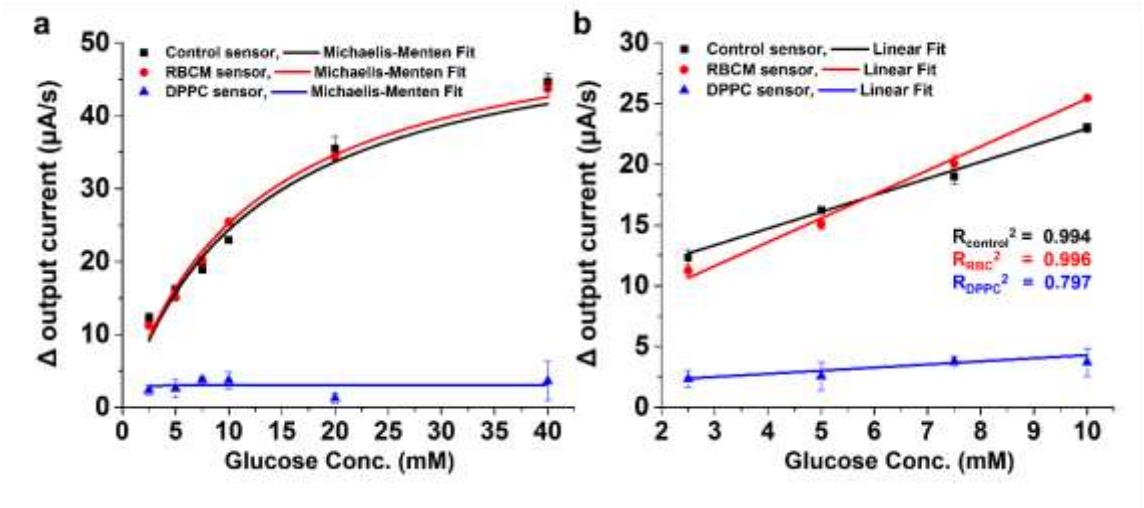

Fig. 4. a) Plot of output current vs. glucose concentration (2.5 to 40 mM) with uncoated, RBCM, and DPPC sensors. The data were fitted by the Michaelis-Menten equation. b) Linear calibration curves in a particular glucose concentration range (2.5 to 10 mM). Each data point represents triplicate measurements.

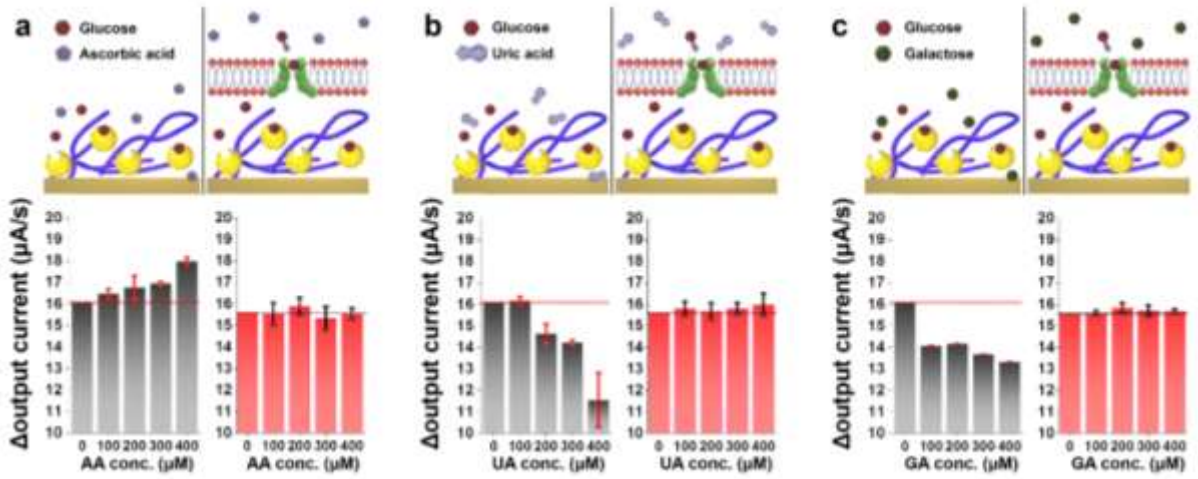

Fig. 5. Selectivity test of RBCM sensor against a) AA, b) UA, and c) GA. The top of each panel displays a schematic illustration of the independent experiment. In each experiment, the glucose concentration was fixed at 5 mM, while the concentration of interfering molecules (AA, UA, and GA) was varied from 0 to 400 μM. The black and red bars represent the uncoated and the RBCM sensor, respectively. Each data point represents triplicate measurements.

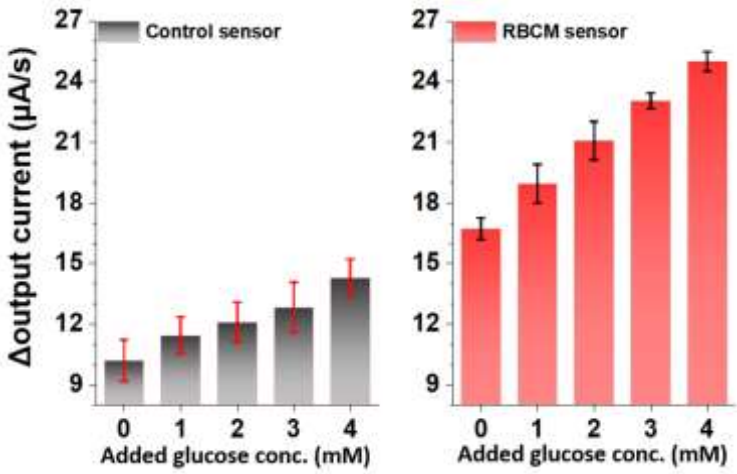

Fig. 6. Selectivity test of the RBCM sensor in human serum with glucose. The pure serum is represented as zero of glucose concentrations. The glucose concentrations added to serum were 1 to 4 mM. Each data point represents triplicate measurements.

highlights

The red blood cell membrane (RBCM) was collected from human whole blood.

The obtained RBCM was employed as a diffusion barrier except for glucose via glucose transporter.

The RBCM-coated sensors were well optimized with the thickness of RBCM for adequate permeability.

The biosensor showed good selectivity for glucose detection under serum and glucose-added serum.